NURETH14-264

HYDRODYNAMIC EFFECTS OF S-CO₂ PROPERTY VARIATIONS IN NUCLEAR ENERGY SYSTEMS

Michael Z. Podowski and Tara Gallaway

Center for Multiphase Research Rensselaer Polytechnic Institute 110 8th St., Troy, NY 12180

Abstract

Supercritical carbon dioxide (S-CO₂) is a very promising material for a variety of industrial applications, including but not limited to, energy conversion systems. The purpose of this paper is to overview recent advancements in the state-of-the art thermo-fluid sciences of supercritical fluids, and their application in the analysis of future S-CO₂ nuclear energy systems. Two specific issues will be discussed in detail. One such issue is concerned with the effect of fluid property variations at near-supercritical pressures on the dynamics of energy systems. In particular, a review is given of several aspects of the modeling of flow-induced oscillations at supercritical pressures and new nondimensional stability maps are presented.

The other issue deals with the analysis of local flow and heat transfer in fluids at supercritical pressures. The impact is discussed of using a mechanistic modeling framework for the coupled fluid mechanics and thermal phenomena on the predictive capabilities of computational models used for system design and optimization purposes. The overall analysis is illustrated using recent results of model testing and validation.

Introduction

Substantial potential benefits have already been identified [3] of using S-CO₂ as working fluid for energy transport in nuclear systems. They include, but are not limited to: high efficiency energy conversion, compact turbomachinery, and the fact that CO₂ is widely available. However, several issues are yet to be resolved to make the S-CO₂ thermodynamic cycle a mature technology for application in future nuclear power plants and other energy conversion systems.

The first part of this paper is concerned with an overview of recent advancements in the state-of-the art thermo-fluid sciences of supercritical fluids, and their application in the analysis of future supercritical nuclear energy systems, including but not limited to S-CO₂. Although in energy system components using working fluids (such as water and CO₂) operating at pressures slightly above critical there is no phase change, the fluid properties still undergo significant variation [7, 17]. In particular, the fluid density decreases by a factor of six or more with increasing temperature around the pseudo-critical point. It has been seen in two-phase flow systems that variations in fluid density can lead to density-wave oscillations, which may cause many undesired problems in system's performance [16]. Thus, similar

issues must be addressed for flows at supercritical conditions. The majority of stability studies to date for supercritical water systems have been performed using simplified models [21, 12], and their results are often not fully consistent and incomplete. The objective of the present paper is to discuss the methodology for, and present the results of, the analysis of density-wave oscillations in heated channels cooled using supercritical fluids. The results of parametric testing and validation of the proposed model are discussed, including a sensitivity analysis to major modeling assumptions. These results include comparisons between time-domain integration of the governing equations, and the frequency-domain analysis using two different approaches to quantify the effect of axial distributions of: fluid properties, power distribution and transient heat transfer across fuel elements. Newly developed SCWR stability maps are also shown.

The second part of this paper deals with the effect of local property variations of multidimensional flow and heat transfer phenomena in supercritical fluids and on the predictive capabilities of computational models used for system design and optimization purposes.

1. Overview of Flow-Induced Oscillations and Instabilities in Heated Channels of Supercritical Fluid Systems

A starting point in the analysis of flow-induced instabilities using any fluid flow model is concerned with determining the dominant mode (or modes) of possible flow oscillations [16]. Instability models in two-phase flow systems can be classified using several different criteria. Based on the temporal character of system response, two kinds of instabilities have been observed: static (excursive) or dynamic (oscillatory). In terms of the governing physical phenomena (and, also, the frequency of oscillations), the following categories can be identified: pressure-drop instabilities (slow), density-wave instabilities (intermediate), and acoustic instabilities (fast). The mode of flow-induced instabilities of particular interest in nuclear reactor technology deals with the neutronically-coupled density wave instabilities (the limiting case of which may assume the form of Ledinegg excursive instabilities), possibly coupled with pressure-drop instabilities.

An important criterion for establishing appropriate boundary conditions for the governing differential equations is associated with the geometrical configuration of the part the system where the unstable oscillations are likely to be originated. For a typical boiling loop with parallel heated channels, shown in Figure 1, two major instability models are: (a) loop-wide oscillations, and (b) oscillations that are practically limited to the heated channels only.

If the total number of parallel channels is large, and only one (or a small fraction of the total number) of them are susceptible to oscillations, the pressure drop across all the channels will be controlled by the stable channels and, thus, will stay approximately constant. Such situation is similar to flow oscillations in a heated channel (or channels) connected in parallel to an unheated bypass that maintains a constant pressure drop across the channel(s). This is shown if Figure 2(a). The corresponding instability mode is known as parallel-channel instabilities, in which the channel pressure drop is the controlled parameter, and the channel inlet flow rate is the variable representing system response. On the other hand, if the number of parallel channels (or the number of groups of identical channels) is small, the total inlet

flow rate becomes the controlled parameter, whereas flow oscillations between the channels are coupled via a common (but no longer constant) pressure drop. This mode of oscillations is called channel-to-channel instabilities. This is shown in Figure 2(b).

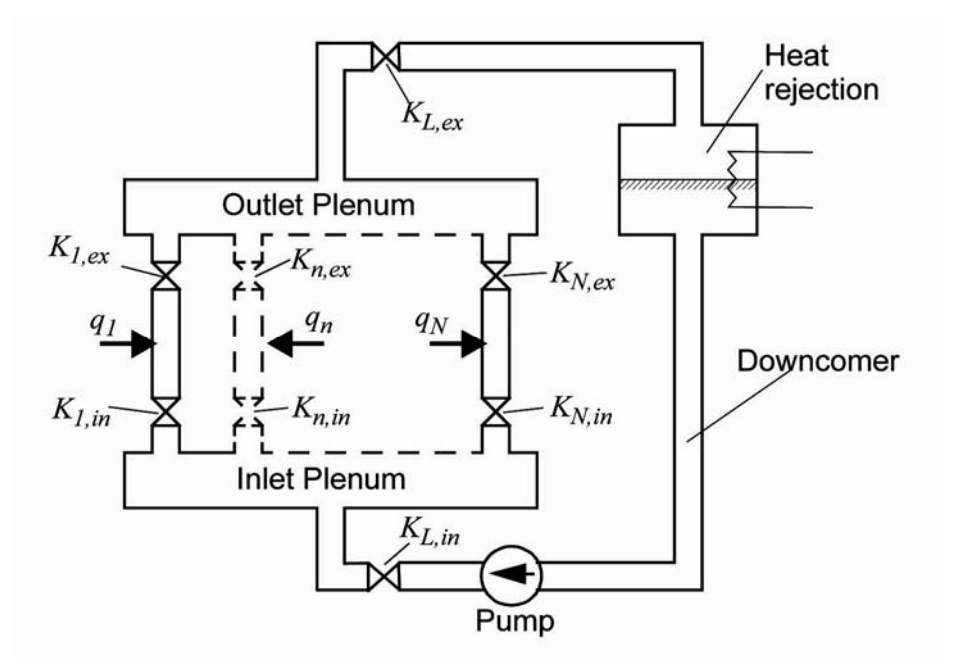
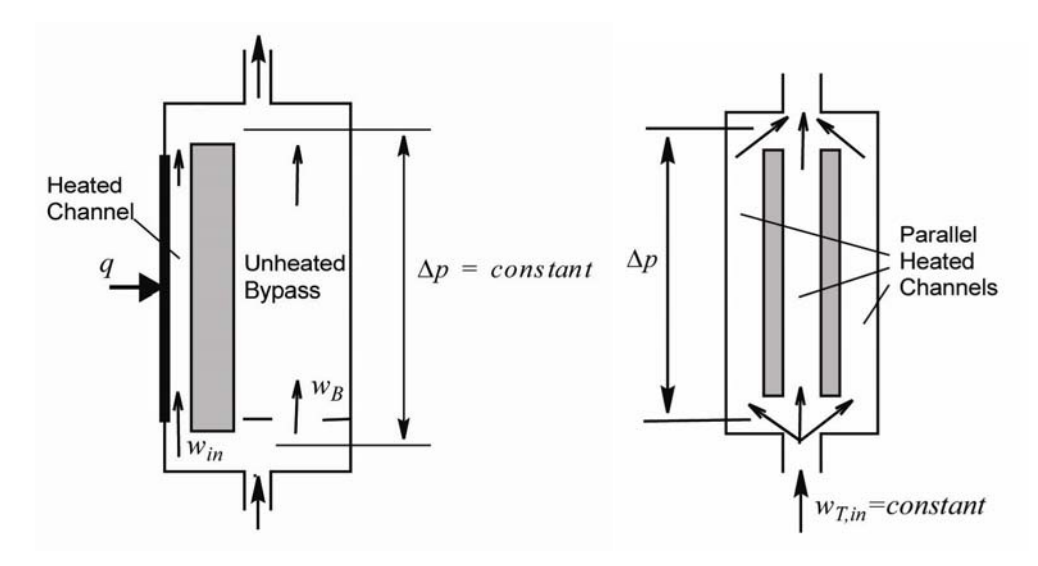


Figure 1. A closed loop system with parallel heated channels



- (a) Parallel-channel oscillations
- (b) Channel-to-channel oscillations

Figure 2. Schematics illustrating the parallel-channel and channel-to-channel instability modes.

Flow-induced instabilities may occur in system components consisting of heated channels combined in a series with unheated channels. Two examples are shown in Figure 3, where the

heated-channel/adiabatic-riser combination in Figure 3(a) illustrates the reactor-core/chimney structure in BWRs, whereas the heated-channel/adiabatic-downcomer combination in Fig. 3(b) corresponds to some of the proposed SCWR designs. A common factor in both cases is that the possible system instabilities are driven by a similar boundary condition, e.g., a common inlet pressure and exit pressure, both established by a large number of stable parallel combined heated/unheated channels representing individual lateral zones of the reactor.

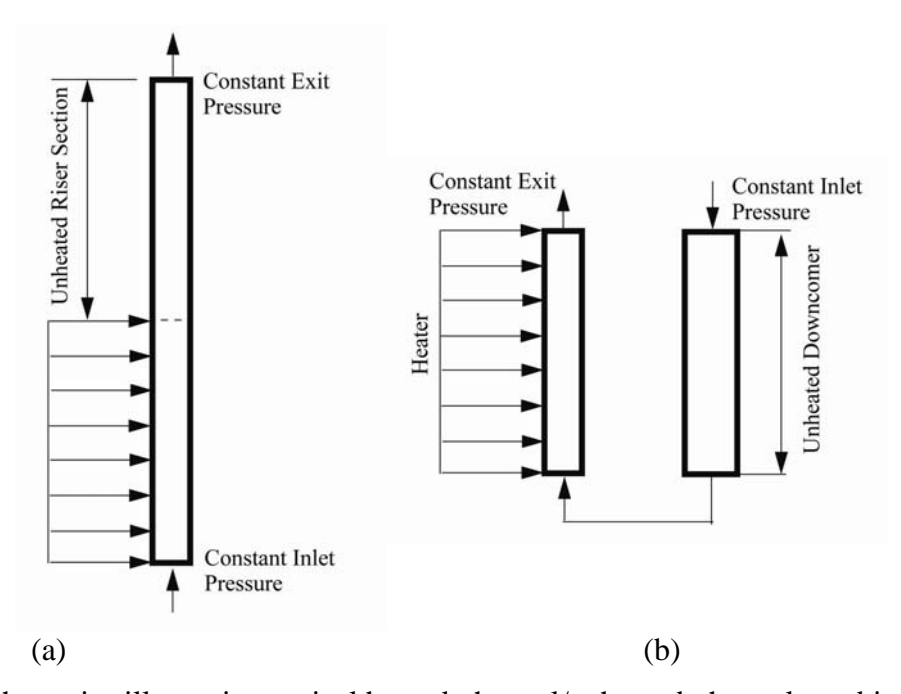


Figure 3. Schematics illustrating typical heated-channel/unheated-channel combinations.

The physical mechanisms behind flow-induced density-wave instabilities are associated with the changes of fluid properties along the flow in heated channels. In the case of BWRs, the effect of boiling causes a gradual change of the average properties of the steam/water mixture. In the case of SCWRs, a similar effect is caused by the changes in properties of (single-phase) water with temperature. As shown in Figure 4, these changes are quite dramatic at pressures slightly above critical.

Depending on the formulation of the governing equations, two major classes of models can be identified: full nonlinear models and linear models. Considering the method of solutions, the two major approaches are: a linearized frequency-domain method [13, 22] and a time-domain method [5, 19, 14, 22]. The former method typically uses linear models, although methods of nonlinear frequency-domain analysis of nuclear reactors have also been developed [15].

The quantitative nature of the frequency-domain method, and its accuracy and computational efficiency, make this approach a very attractive tool for evaluating stability-imposed limits on system operation, including both the marginal stability conditions and the available stability margins for any given steady-state operating conditions. The range of applications of such models and the accuracy of their predictions depend on how well they capture the physical phenomena governing transient fluid flow and heat transfer.

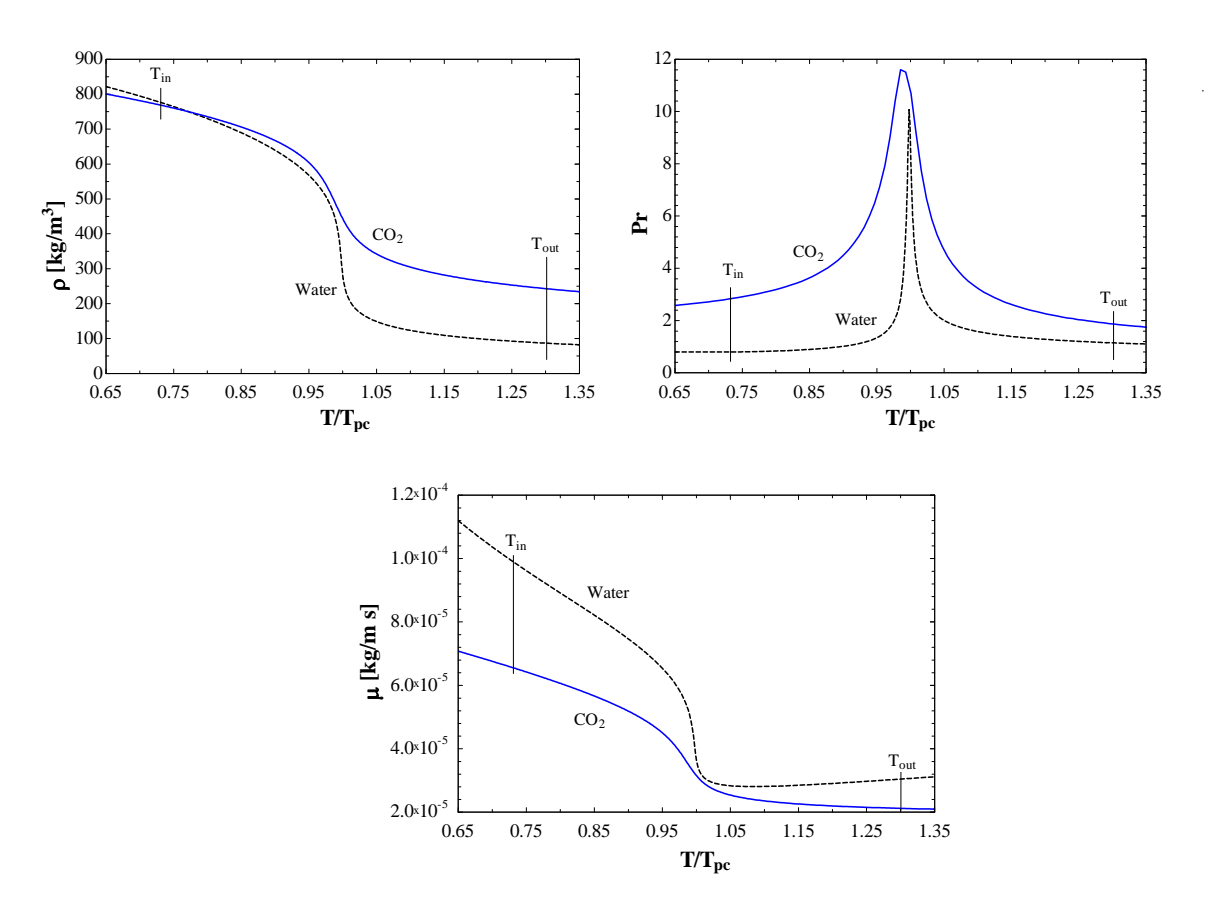


Figure 4. Illustration of the temperature-dependence of supercritical water properties at 25 MPa.

Whereas theoretical methods of nonlinear system analysis, including but not limited to the frequency-domain approach [11, 16] are capable of providing interesting insight into the nature of instabilities and identifying the so-called stability islands for simple models, the analysis of dynamics and stability of complex parallel-channel reactor systems is normally based on time-domain solutions obtained from direct numerical integration of the governing equations of two-phase flow and heat transfer. It is important to realize that although time-domain codes do not bear any theoretical limitations, such an approach typically requires tedious computations the results of which are associated with substantial uncertainties and require extensive testing and assessment.

2. One-Dimensional Model of Supercritical Fluid Dynamics

The time dependent one-dimensional conservation equations of mass, momentum and energy, respectively, for a single-phase fluid with variable properties can be written as

$$\frac{\partial \rho}{\partial t} + \frac{\partial G}{\partial z} = 0 \tag{1}$$

$$\frac{\partial G}{\partial t} + \frac{\partial \left(\frac{G^2}{\rho}\right)}{\partial z} = -\frac{\partial p}{\partial z} - \frac{f}{2d} \frac{G^2}{\rho} - \rho g - K_{in} \frac{G_{in}^2}{2\rho_{in}} \delta(z) - K_{out} \frac{G_{out}^2}{2L\rho_{out}} \delta(z - L)$$
(2)

$$\frac{\partial(\rho h)}{\partial t} + \frac{\partial(Gh)}{\partial z} = \frac{q'' P_h}{A_c} \tag{3}$$

where $\delta(z)$ in Eq.(2) is the Dirac's Delta Function.

Whereas Eqs.(1)-(3) are nonlinear from a mathematical point of view, they can be linearized for the purpose of stability analysis. Namely, for stable systems, small perturbations in external perturbations (such as the total pressure drop) will result in small perturbations in other fluid parameters (such as mass flux and enthalpy) from their steady-state values. Thus, the individual time- and position-dependent variables can be expressed as combinations of their steady-state values and the corresponding fluctuating components (which are also time-and position-dependent)

$$G(z,t) = G_{ss} + \delta G(z,t) \tag{4}$$

$$h(z,t) = h_{ss}(z) + \delta h(z,t) \tag{5}$$

The next step is to substitute Eqs.(4) and (5) into Eqs.(1)-(3), and ignore higher order perturbation terms. It is important to recognize that the linearization process must include the temporal and spatial variations of fluid properties. The fluctuations in practically all properties can be expressed as functions of the enthalpy perturbation. For example, the density perturbation can be written as

$$\delta \rho(z,t) = \frac{d\rho}{dh} \bigg|_{z=0} \delta h(z,t) \tag{5}$$

Naturally, the properties of supercritical fluids also dependent on pressure (which varies along the flow). However, this dependence is at least one order of magnitude smaller compared to the dependence on enthalpy, and can be neglected. On the other hand, the accuracy of model predictions will be strongly affected by any inaccuracies in the values of property derivatives (such as $d\rho/dh|_{ss}$ in Eq.(5)). Thus it is very important that those derivatives be accurately determined from the property tables. The required level of accuracy can be achieved by using analytical formulas such as those introduced by Gallaway et al. [7]

$$\zeta(T,p) = a_{\zeta,i}(P) + b_{\zeta,i}(P)T + c_{\zeta,i}(P)T^{2} + d_{\zeta,i}(P)T^{3}$$
for $T_{i} \le T \le T_{i+1}$ $(i = 1, 2, ..., K)$ (6)

The values of various properties evaluated from Eq.(6) are shown in Fig. 4. As can be readily noticed, they can hardly be distinguished from the directly tabulated values. What is particularly important, the use of Eq.(6) allows one to analytically evaluate the needed derivatives of the individual properties. Examples of the derivatives of density and viscosity of supercritical water with respect to temperature are shown in Fig. 5.

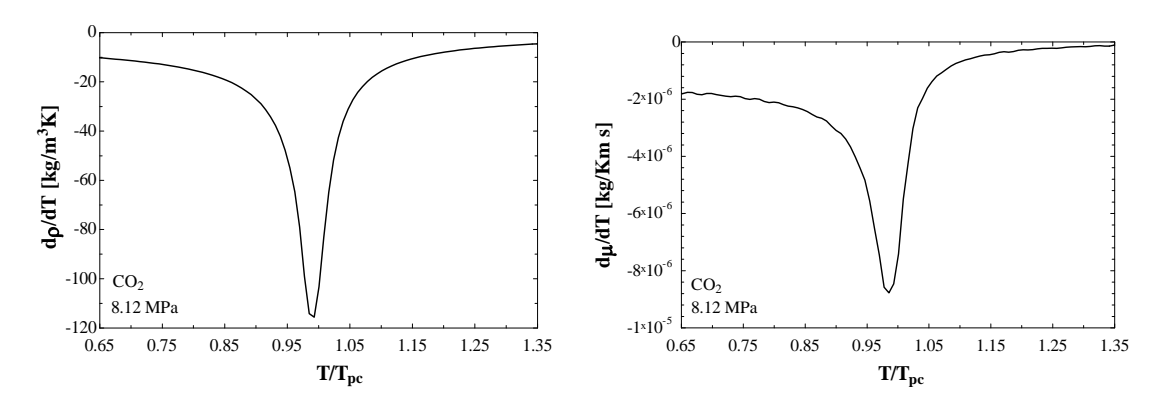


Figure 5. Illustration of the temperature-dependence of property derivatives for supercritical water at 25 MPa.

Various solution methods can be used to study stability the systems described by linearized Eqs.(1)–(3). A traditional approach is to nodalize/discretize the model, thus replacing the governing partial differential equations by a system of ordinary differential equations. Summing up the resultant partial pressure drops along the channel and rearranging, the momentum equation becomes

$$\frac{dx_0}{dt} = \sum_{i=1}^{N} \alpha_i y_i + \beta x_0 + \psi \delta \Delta p \tag{7}$$

where $x_o(z,t) = \delta G_{in}(z,t)$, and $y_i(t) = \delta h(z_i,t)$. The individual nodal enthalpy perturbations can be expressed in terms if the inlet flow rate perturbation as

$$\frac{dy_i}{dt} = \sum_{j=1}^{i} \gamma_{i,j} y_j + \lambda_i x_0 \tag{8}$$

For any given external perturbation in the channel pressure drop, the system of equations, Eqs.(7)-(8) can be integrated numerically in the time domain to evaluate the corresponding inlet mass flux perturbation. Alternatively, Eqs.(7)-(8) can be Laplace-transformed and used to evaluate the transfer function for a discretized system

$$H_{dis}(s) = \frac{\mathcal{I}\left\{\delta\hat{G}_{in}(s)\right\}}{\mathcal{I}\left\{\delta\Delta\hat{P}(s)\right\}} = \frac{\sum_{m=0}^{M} b_m s^m}{\sum_{n=0}^{N} a_n s^n}$$

$$\tag{9}$$

It turns out, however, that a different approach, free of any nodalization and computational errors, can also be used by applying the Laplace-transform directly to the governing partial differential equations and taking advantage of the fact that the resultant equations constitute a system of ordinary differential equations with respect to the spatial coordinate, z. Specifically, integrating the momentum equation over the length of the channel and using the appropriate expansions and substitutions, yields the following equation

The 14th International Topical Meeting on Nuclear Reactor Thermalhydraulics, NURETH-14 Toronto, Ontario, Canada, September 25-30, 2011

$$\frac{d}{dt} \int_{0}^{L} x dz + \frac{2G_{ss}}{\rho_{ss,out}} x_{L} - \frac{G_{ss}^{2} A_{L}}{\rho_{ss,out}^{2}} y_{L} - \frac{2G_{ss}}{\rho_{ss,in}} x_{0} = \delta \Delta p - \int_{0}^{L} \left[C_{1}(z) x + C_{2}(z) y \right] dz$$

$$-g \int_{0}^{L} (A(z) y) dz - K_{in} \frac{G_{ss}}{\rho_{ss,in}} x_{0} - K_{out} \left(\frac{G_{ss}}{\rho_{ss,out}} x_{L} - \frac{G_{ss}^{2} A_{L}}{2\rho_{ss,out}^{2}} y_{L} \right) \tag{10}$$

where $x_L(t) = \delta G(L,t)$.

Using the Laplace-transforming concept and rearranging, the following equations can be derived

$$\frac{d^2\hat{X}_R}{dz^2} - \beta \frac{d\hat{X}_R}{dz} - \alpha(z)\omega \frac{d\hat{X}_I}{dz} + \gamma(z)\omega \hat{X}_I = 0$$
(11)

$$\frac{d^2\hat{X}_I}{dz^2} + \alpha(z)\omega \frac{d\hat{X}_R}{dz} - \beta \frac{d\hat{X}_I}{dz} - \gamma(z)\omega \hat{X}_R = 0$$
 (12)

where $\hat{X}(s,z) = \mathcal{I}\{x(t,z)\}\$ for $s = j\omega$, and $\hat{X}(j\omega) = \hat{X}_R(\omega) + j\hat{X}_I(\omega)$.

Eqs.(11)-(12) can be integrated for any given ω . Substituting the resultant expressions to Eq.(15), yields a rigorous, equivalent to exact analytical, solution for the characteristic function of the system

$$G(j\omega) = \frac{\mathcal{I}\left\{\delta\hat{G}_{in}(j\omega)\right\}}{\mathcal{I}\left\{\delta\Delta\hat{P}(j\omega)\right\}} = \operatorname{Re}G(\omega) + j\operatorname{Im}G(\omega)$$
(13)

Eq.(19) can be used directly to obtain the Nyquist locus for the system and, thus, to evaluate the stability characteristics of the system which are free of any computational errors and inaccuracies. Typical predictions for the geometries and operating conditions similar to those for future SCWRs are discussed in the next section.

3. Overview of Stability Analysis Results

The solution methods developed in the previous sections are first compared against each other for the default flow conditions shown in Table 4-1, considering a square fuel assembly.

Table 4-1: Default Flow Conditions for Stability Model Testing Using Water	
Inlet Temperature	280°C
System Pressure	25 MPa
Mass Flux	746 kg/m ² s
Inlet/Outlet Loss Coefficients	10/1
Thickness of Heater	0.2 mm
Heat Transfer Coefficient	Bishop Correlation [2]

In the time-domain analysis, a small short-lasting perturbation to the channel pressure drop, has been used as the forcing function. Naturally, the calculated asymptotic system response

under a constant-pressure-drop boundary condition is independent of the original shape of this perturbation. A typical response of the inlet mass flux to this pressure drop perturbation in the time domain is shown in Fig. 6.

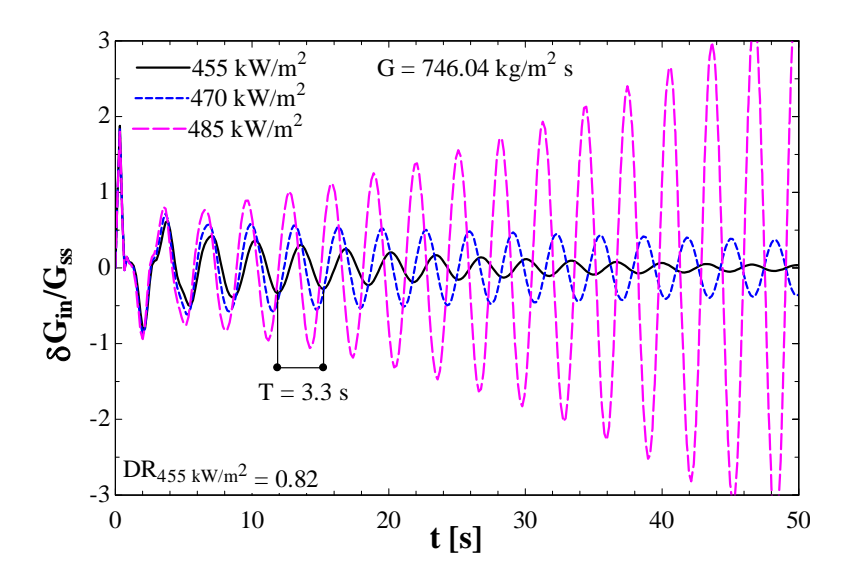


Figure 6. Time domain results for various channel operating conditions.

Based on the parametric studies that have been performed, it turns out that the minimum number of nodes to obtain full convergence level is between 40 and 50 axial nodes, but an acceptable accuracy is already reached for about 30 nodes. As the heat flux is increased at a fixed flow rate, the stability boundary is gradually approached and exceeded. Fig. 6 shows that the heat flux corresponding to marginal stability conditions is about 470 [kW/m²].

Fig. 7 shows the frequency-domain predictions for the same system and operating conditions, using two integration methods of the governing equations: one is based on the nodal model and the other on a rigorous integration of the distributed-parameter model. In this figure, $s = j\omega$, where ω ranges from 0 to 3 [rad/s]. It can be seen that the results are consistent with the time-domain predictions. Specifically, the plot which does not encircle the origin (for $q'' = 455 \text{ [kW/m}^2\text{]}$) corresponds to stable conditions, whereas the one that encircles the origin ((for $q'' = 485 \text{ [kW/m}^2\text{]}$) refers to unstable conditions. Furthermore, the Nyquist plot crosses the origin at a heat flux value slightly higher than 470 [kW/m²], which confirms, in a more accurate manner, the time-domain result.

It is important to mention that the frequency domain method allows one to directly determine the natural frequency of oscillations for a wide range of system's operating conditions. In the present case, the predicted natural frequency for the case at marginal stability was, $\omega = 1.9$ [rad/s], which corresponds to the oscillation period in the time domain for the same case, $T = 2\pi/\omega = 3.3$ [s].

As it can be seen, the frequency domain solution for the discretized channel model agrees well with the exact solution over the range of frequencies slightly above the natural frequency of

oscillations. The fact that the former model's solution gradually diverges from the exact solution at higher frequencies is mainly due to truncation errors and other numerical inaccuracies associated with evaluating the values of high-order polynomials.

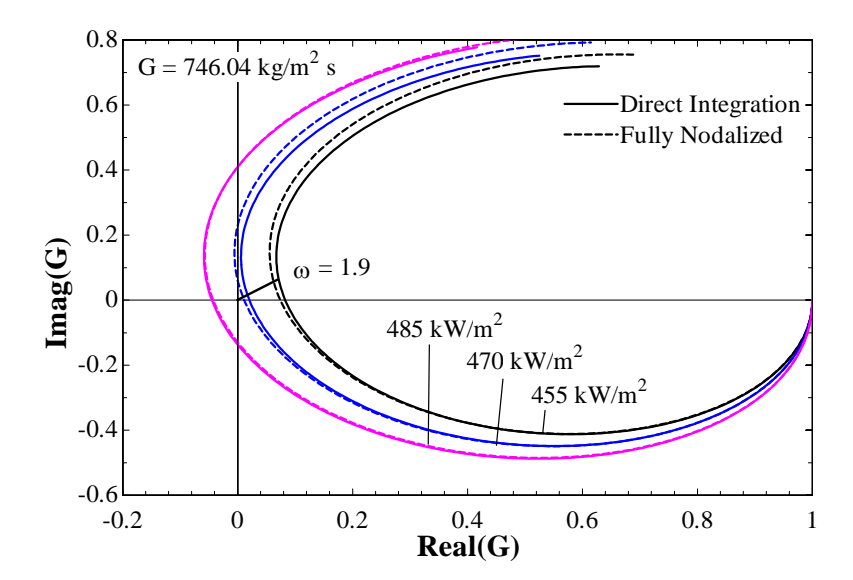


Figure 7. Frequency domain results for various channel operating conditions.

The results presented thus far can be generalized by formulating stability maps which show the marginal stability conditions for various channel operating conditions. Two such maps are shown in Fig. 8.

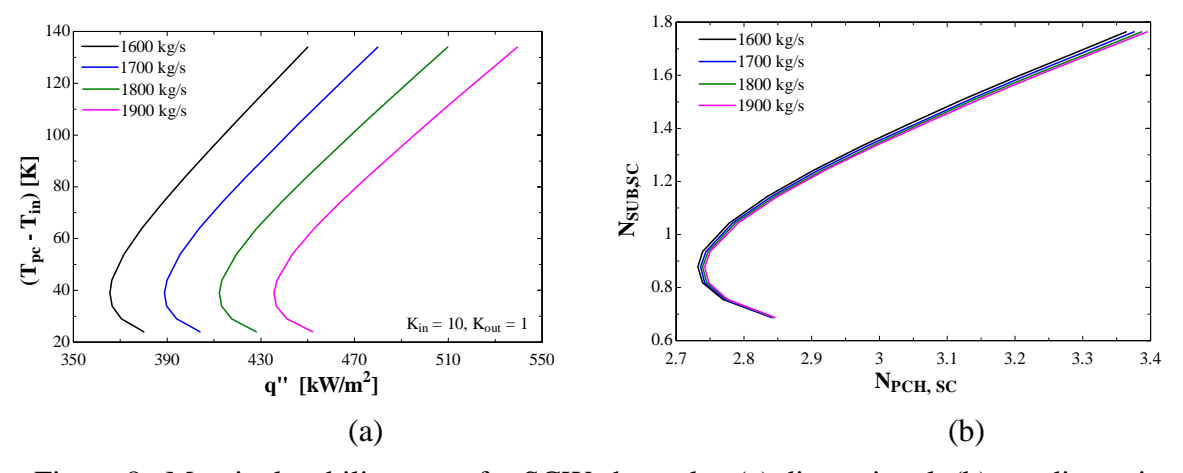


Figure 8. Marginal stability maps for SCW channels: (a) dimensional, (b) nondimensional where $N_{SUB,SC} = \frac{h_{pc} - h_{in}}{\Delta h_{ref}}$ and $N_{PCH,SC} = \frac{q}{w\Delta h_{ref}}$.

Fig. 8(a) shows a dimensional map, given in terms of inlet "subcooling" (i.e., the difference between the pseudo-critical temperature and the inlet temperature) as a function of wall heat flux. As can be seen the marginal stability lines for different coolant mass flow rates are distinctively different from one other.

The map in Fig. 8(b) has been formulated in terms of a nondimensional inlet "subcooling" vs. a nondimensional power-to-flow ratio. In this case the individual curves for different mass flowrates almost collapse on the top of one another. This result is consistent with the corresponding stability maps for boiling channels, where single curves are obtained for simple models (eg., HEM) of two-phase flow, whereas slightly different curves are obtained for more detailed models (such as those which account for subcooled boiling).

3.1. Parametric Study

To evaluate the effect of local pressure losses on the stability of a heated SCW channel, parametric calculations have been performed for different inlet and exit loss coefficients. The results are shown in Fig. 9. It can be seen that as the inlet loss coefficient increases, the system becomes more stable. Conversely, as the outlet loss coefficient increases the system becomes more unstable. These trends are consistent with those observed in boiling channels.

Since the axial power distribution along reactor coolant channels is highly nonuniform, it is important to evaluate the effect of power profile on system stability. Specifically, a chopped cosine distribution can be used for this purpose, given by

$$q''(z) = q''_{\text{max}} \cos\left(\pi \frac{z - L/2}{L_e}\right) \tag{20}$$

where $L_e = L + 2\Delta L$ is the extrapolation distance.

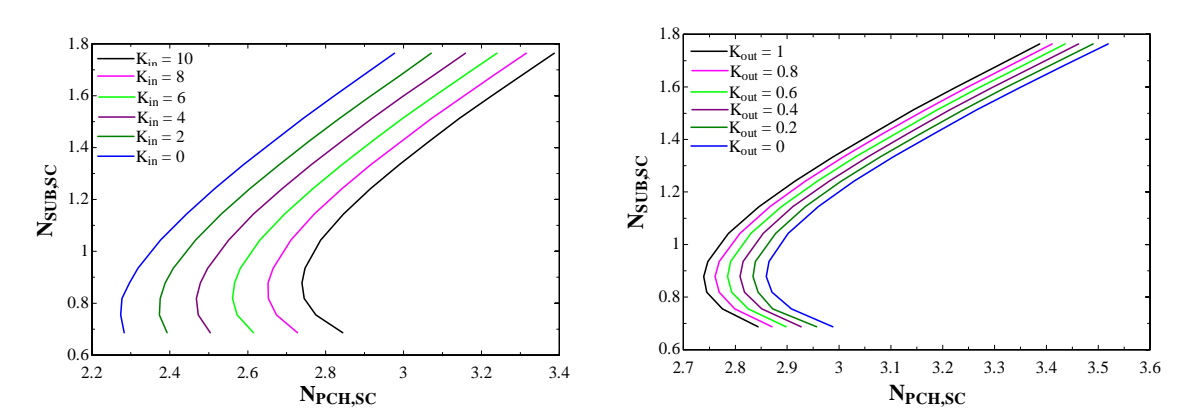


Figure 9. Effect of local loss coefficients on SCW channel stability where $N_{SUB,SC} = \frac{h_{pc} - h_{in}}{\Delta h_{ref}}$

and
$$N_{PCH,SC} = \frac{q}{w\Delta h_{ref}}$$
.

The results of a parametric study performed by varying the $\Delta L/L$ ratio from 100 (which practically corresponds to a uniform power profile) down to 0 (the case with no extrapolation) are shown in Figure 10. It can been seen that as the departure from a uniform distribution increases, the system becomes more stable. Thus, one concludes that the neutronics-driven nonuniform reactor axial power profile has a stabilizing effect on flow induced oscillations.

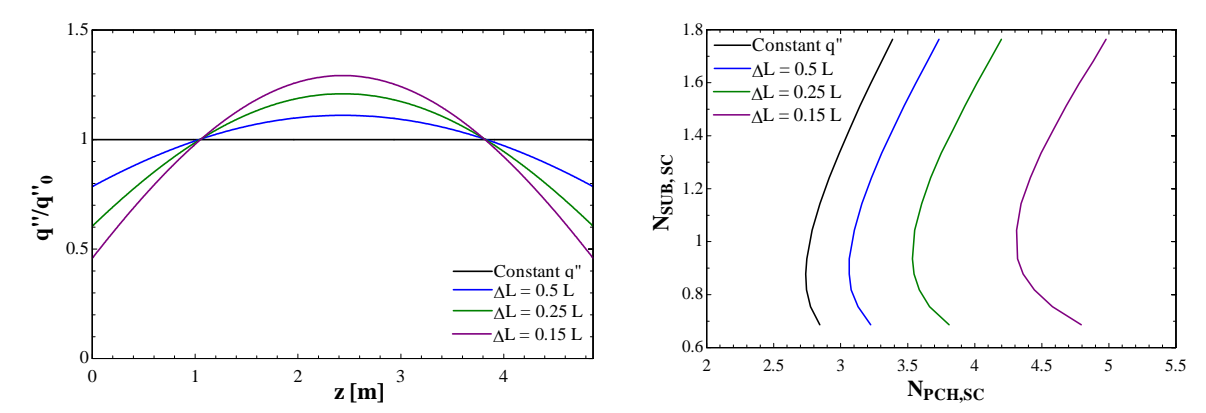


Figure 10. Effect of axial power distribution on SCW channel stability where

$$N_{SUB,SC} = \frac{h_{pc} - h_{in}}{\Delta h_{ref}}$$
 and $N_{PCH,SC} = \frac{q}{w \Delta h_{ref}}$.

Thermal storage in the fuel rods will effect the overall stability of the system as well. A default heater thickness of 0.2 mm has been assumed thus far in the analysis. This value is varied to show the effect of the thickness of the heater on the stability of the system in Figure 11. From this figure it is seen that as the heater thickness, t, is increased, the system becomes more stable.

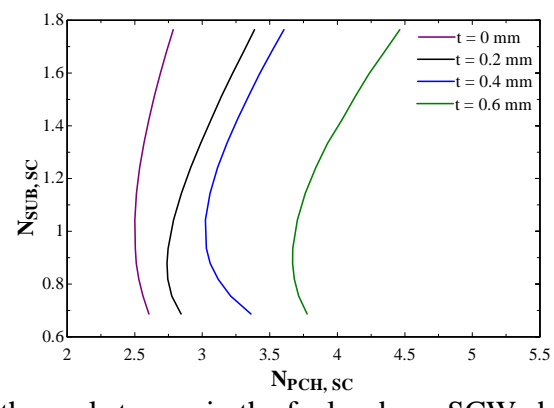


Figure 11. Effect of thermal storage in the fuel rods on SCW channel stability where

$$N_{SUB,SC} = \frac{h_{pc} - h_{in}}{\Delta h_{ref}}$$
 and $N_{PCH,SC} = \frac{q}{w\Delta h_{ref}}$

3.2. Comparison against other results

As a part of model testing and validation, the results obtained using the present model have been compared against the stability predictions shown by Pandey and Kumar [12] in Figure 12. The comparison revealed that simple models, such as that proposed by Pandey and Kumar [12] may significantly underestimate the onset of instability conditions and provide non-conservative estimates of the SCWR stability limits. Naturally, what is still needed is a validation of the current model against actual experimental data.

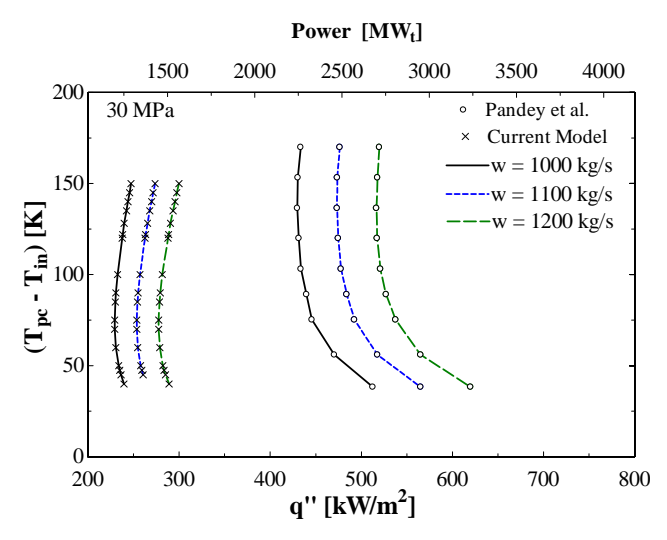


Figure 12. Comparison of the current work to the Pandey and Kumar stability analysis [12].

The current stability analysis was also compared to the Ortega Gomez stability analysis, which was developed based on similarities between instabilities known to occur in multiphase flow and expected instabilities in flow at supercritical conditions [18]. A comparison between these works is seen in Fig. 13.

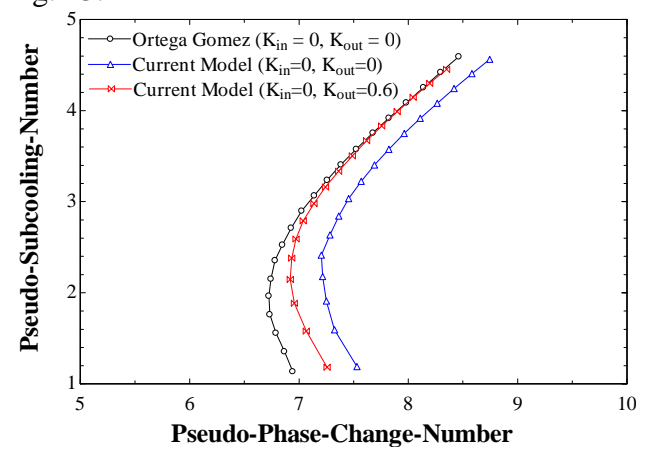


Figure 13. Comparison of the current work to the Ortega Gomez stability analysis [18].

4. Conclusions

Fluids at supercritical conditions offer great benefits for use as a reactor coolant in future Gen. IV reactors. However, several hydrodynamic issues specific to fluid properties must be addressed and understood before these reactor designs become viable. Stability is one of such

issues. In this study, two different methods of stability analysis have been introduced for systems cooled using fluids at supercritical pressures: a time-domain method and a frequency-domain method. Furthermore, two methods of solution for the frequency-domain approach have been developed: a rigorous (exact) integration method and a multi-node approximation. It has been demonstrated that both methods of solution give similar results concerning the stability characteristics of SCW heated channels for the conditions corresponding the operating conditions of the proposed supercritical water reactors (SCWRs) in the range of natural frequency of oscillations. It has also been shown that the results of the time-domain integration method approximate the exact solution with a good accuracy.

5. References

- 1. Bejan, A., Convective Heat Transfer 3rd Edition, John Wiley, 2004.
- 2. Bishop, A. A., Sandberg, R. O., and Tong, L. S., "Forced Convection Heat Transfer to Water Near Critical Temperatures and Supercritical Pressures," *WCAP-2056-P, Part-III-B*, 1964.
- 3. Buongiorno, J. and MacDonald, P.E., (2003), "Supercritical Water Reactor Progress Report for the FY-03 Generation-IV R&D Activities for the Development of the SCWR in the U. S.", *INEEL/EXT-03-01210*, INL.
- 4. Chien, K. Y., "Predictions of Channel and Boundary Layer Flows with a Low Reynolds Number Turbulence Model," *AIAA*, 20(1):33-38, 1982.
- 5. Dykhuizen, R. C., Roy, R. P. and Kalra, S. P. (1986, 'A Linear Time-Domain Two-Fluid Model Analysis of Dynamic Instability in Boiling Flow Systems', *J. Heat Transfer*, 108, pp. 100-108.
- 6. Favre, A., <u>Problems of Hydrodynamics and Continuum Mechanics</u>, "Statistical Equations fo Turbulent Gases," Philadelphia, SIAM, 1969.
- 7. Gallaway, T., Antal, S.P. and Podowski, M.Z. (2008), "Multidimensional Model of Fluid Flow and Heat Transfer in Generation-IV Supercritical Water Reactors", *Nuclear Engineering & Design*, 238.
- 8. Gallaway, T., "Modeling of Flow and Heat Transfer for Fluids at Supercritical Conditions," *Ph.D. Thesis*, Rensselaer Polytechnic Institute, 2011.
- 9. Kataoka, K. (2002), "Development Project of Supercritical Water Cooled Power Reactor", Proceedings of ICAPP-2002, Hollywood, Florida.
- 10. Kim, H., Bae, Y. Y., Kim, H. Y., Song, J. H., and Cho, B. H., "Experimental Investigation on the Heat Transfer Characteristics in a Vertical Upward Flow of Supercritical CO₂," *Proc. of ICAPP*, 2006.
- 11. Lahey, R.T., Jr. and Podowski, M. Z. (1988), "On the Analysis of Instabilities in Two-Phase Flow", *Multiphase Science and Technology*, **4**, Hemisphere Publishing Corp. .
- 12. Pandey, M. and Kumar, M.A. (2008), "Analysis of Coupled Neutronic-Thermohydraulic Instabilities in Super-critical Water-Cooled Reactor by Lumped Parameter Modeling", *ICONE 16*, Paper 48407.

- 13. Peng, S. J., Podowski, M. Z., Lahey, R. T. Jr., and Becker, M. (1984), NUFREQ-NP, A Computer Code for the Stability Analysis of Boiling Water Nuclear Reactors, *Nucl. Sci. Eng.* 88, pp. 3-12.
- 14. Pinheiro Rosa, M. and Podowski, M.Z. (1994), "Nonlinear Effects in Two-Phase Flow Dynamics", *Nuclear Engineering and Design*, **146**, pp. 277 -288.
- 15. Podowski, M.Z. (1986), "Nonlinear Stability Analysis for a Class of Differential-Integral Systems Arising from Nuclear Reactor Dynamics", *IEEE Transactions on Automatic Control*, Vol. AC-31, No. 2.
- 16. Podowski, M.Z. (1992), "Instabilities in Two-Phase Systems", in *Boiling Heat Transfer*, Elsevier Publishing Corp.
- 17. Podowski, M.Z., (2008), "Thermal-Hydraulic Aspects of SCWR Design", *Journal of Power and Energy Systems*, **2**, 1.
- 18. Ortega Gomez, T., "Stability Analysis of the High Performance Light Water Reactor," *PhD Thesis*, Universitat Karlsruhe, 2009.
- 19. Rizwan-Uddin and Dorning, J. J. (1986), "Some Nonlinear Dynamics of a Heated Channel", *Nucl. Eng. Design*, 93, pp. 1-14.
- 20. Song, J. H., Kim, H. Y., Kim, H., and Bae, Y. Y., "Heat Transfer Characteristics of a Supercritical Fluid Flow in a Vertical Pipe," *J. Supercrit. Fluids*, 44:164 171, 2008.
- 21. Yi, T.T., Koishizuka, S. and Oka, Y. (2004), "A Linear Stability Analysis of Supercritical Water Reactors (I)", *Journal of Nuclear Science and Technology*, **41**, pp. 1166 1175.
- 22. Zhou, J. and Podowski, M.Z. (2001), "Modeling and Analysis of Hydrodynamic Instabilities in Two-Phase Flow Using Two-Fluid Model", *Nucl. Eng. Des.*, 204, pp. 129-142.